Improvement of Prediction Accuracy of Magnetic Field-Based Positioning with a High-Isolation Relay Circuit

Kouga MIYAJI* and Ai-ichiro SASAKI
Dept. of Electronic Engineering and Computer Science, Kindai University, Higashi-Hiroshima, 739-2116 Japan
*Corresponding author: 2333850003v@hiro.kindai.ac.jp

Abstract – Magnetic field-based positioning (MFP) is expected as a method that can establish accurate indoor positioning systems. With MFP, the position of a target device is predicted based on signals received by multiple sensors located at different points around the target area. A key point for accurate positioning is gathering the multiple sensor signals without degrading their quality. One of simple methods to gather the multiple sensor signals is to use a relay circuit. Since a dynamic range of the sensor signals becomes very large in MFP systems, the isolation performance of the relay circuit greatly influences prediction accuracy of the systems. We fabricated a high-isolation relay circuit and investigated the influences of the isolation performance of the circuit upon prediction accuracy of MFP systems.

Keywords – magnetic field; positioning system; machine learning; neural network; relay circuit

1. Introduction

The demand for indoor positioning technologies has been increasing with the popularization of mobile devices. Currently, methods using radio waves are being actively researched for predicting the position of the devices in indoor environments [1, 2]. However, due to the inherent nature of radio waves, it is difficult to avoid the influences of obstacles such as reflections and attenuation, and the positioning accuracy is degraded by these influences.

On the other hand, if the target area is limited to a short distance on the order of several meters, the approach using magnetic fields, which are less susceptible to obstacles, is considered to be promising in terms of prediction accuracy. Because of this advantage, magnetic field-based positioning (MFP) has also been actively studied [3, 4].

In MFP, magnetic field signals emitted by a mobile device (TX) are received by multiple sensors (RX), and the information of the sensor signals is used to predict the Tx position. We previously demonstrated the effectiveness of machine learning for MFP in terms of both prediction accuracy and computational speed [5, 6]. The advantage of applying machine learning to MFP is that the training data, which are the sensor signals, can be easily obtained by calculation. To take this advantage, good agreement between the calculated and real signals is required. In practice, however, it is difficult to realize complete agreement between them.

In real MFP systems, it is necessary to gather the signals received by multiple sensors. One of simple methods to gather the multiple sensor signals is to use relay circuits. It was revealed by our previous research that the main factor of the disagreement is poor isolation nature of the relay circuits [7].

In this study, we investigated the influence of isolation characteristics of the relay circuits upon prediction accuracy of MFP. Furthermore, we fabricated a circuit with physical contact relays (PCRs) and achieved the isolation ratio of 76 dB. The average prediction error obtained with our MFP system was successfully reduced from 24.6 cm to 5.7 cm by introducing the PCR circuit.

2. MFP System with Machine Learning

Figure 1 shows the configuration of an MFP system used in this study. A transmitter (TX) which generates magnetic fields through a uniaxial coil imitates a target mobile device. The position of the TX is predicted based on the magnetic field signals received by multiple sensors (RX1–4). In our system, four RXs are installed, but not limited to four.

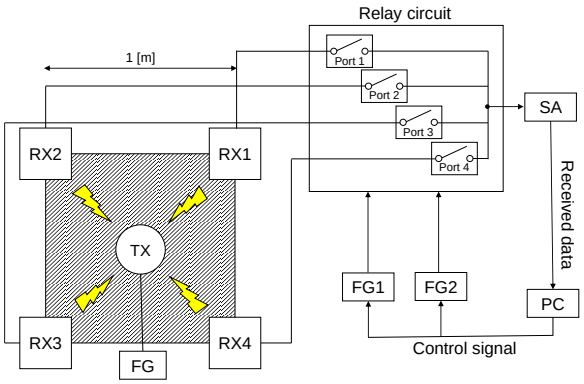

Figure 1. MFP system used in this study.

An AC voltage is applied to the TX from a function generator (FG) to generate magnetic field signals. The signals are received by sensors (RX1–4) placed at four corners of the target area. The four sensor signals are input to a relay circuit, and one of the signals is selected and delivered to a spectrum analyzer (SA). The data signals analyzed by SA are transferred to a PC. It becomes possible to acquire the four sensor signals by switching the relay circuit. The switching operation of the relay circuit is controlled by DC voltage signals generated by function generators (FG1 and FG2). The PC is used for calculating the position of the TX based on the four sensor signals.

Next, we explain the machine-learning approach to MFP systems. As shown in Figure 2, the essence of this approach is generating a predictor function **P** that can output the predicted TX position $\mathbf{r}^{(\mathrm{p})}$ in response to sensor signal information. The superscript (p) means that $\mathbf{r}^{(\mathrm{p})}$ is a predicted position. Obtaining **P** requires a large amount of training data for machine learning. Generally speaking, it is cumbersome and time-consuming to prepare a sufficient number of training data. Fortunately for MFP systems, training data can be computationally obtained, making it easy to prepare a large number of training data.

The training data can be written as

$$\left(B_{\mathrm{calc}}^{(1)}, B_{\mathrm{calc}}^{(2)}, B_{\mathrm{calc}}^{(3)}, B_{\mathrm{calc}}^{(4)}; \mathbf{r}^{(\mathrm{t})}\right), \qquad (1)$$

where $B_{\mathrm{calc}}^{(k)}$ and $\mathbf{r}^{(\mathrm{t})}$ are the calculated values of the received signal of *k*-th RX and the true position of the TX, respectively.

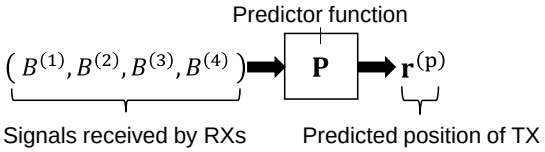

Figure 2. Calculation of TX position by using a predictor function obtained with machine learning.

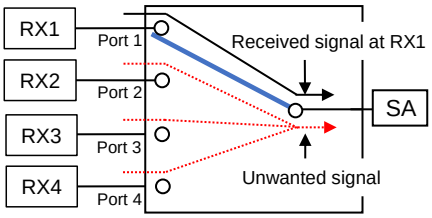

Figure 3. Conceptual diagram of unwanted signal contamination within a relay circuit.

A large number of training data can be prepared easily by calculating $B_{\mathrm{calc}}^{(k)}$ for various $\mathbf{r}^{(\mathrm{t})}$. After machine learning with the training data, we can obtain **P** having the following property.

$$\mathbf{r}^{(\mathrm{p})} = \mathbf{P}\left(B^{(1)}, B^{(2)}, B^{(3)}, B^{(4)}\right) \qquad (2)$$

Here $B^{(k)}$ is the received signal of *k*-th RX. Since $\mathbf{r}^{(\mathrm{p})}$ is the predicted position of TX, it can be regarded as an approximation of the true position $\mathbf{r}^{(\mathrm{t})}$. For evaluating the performance of **P**, we define the prediction error by

$$d \triangleq \left\|\mathbf{r}^{(\mathrm{t})} - \mathbf{r}^{(\mathrm{p})}\right\|_2. \qquad (3)$$

In this study, we used "Wolfram Mathematica 12.0" for machine learning and adopted "Neural Network" as the learning method.

3. Prediction Accuracy and Isolation Characteristics of Relay Circuits

Figure 3 shows a conceptual diagram of unwanted signal contamination that degrades the isolation ratio of relay circuits. In MFP systems, the received signal of each RX is delivered to SA via the relay circuit that switches the route (Port 1–4). Figure 3 shows the situation where the path is connected to Port 1. It is considered that the signal received by RX1 is delivered to SA in this situation. However, in practice, signals received by other sensors are slightly transmitted to SA because of incomplete isolation nature of relay circuits.

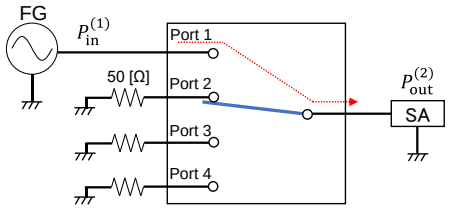

Figure 4. Setup to measure S_{21}.

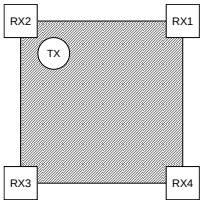

Figure 5. Situation where unwanted signals make the greatest impact on $B^{(4)}$ which is the signal received by RX4.

To quantitatively express the isolation performance of the relay circuit, we define *S*-parameters as

$$S_{ij}\,[\text{dB}] = P_{\text{out}}^{(i)}\,[\text{dBm}] - P_{\text{in}}^{(j)}\,[\text{dBm}], \quad (4)$$

where $P_{\text{in}}^{(j)}$ is the power input to Port j, and $P_{\text{out}}^{(i)}$ is the power delivered to SA when it is connected to Port i. The S_{ij} $(i \neq j)$ represents the degree of the unwanted signal contamination. As an example, the setup to measure S_{21} is depicted in Figure 4. By measuring S_{ij} for all i and j, the isolation performance of the relay circuit can be determined.

In MFP systems, the negative impact brought about by the unwanted signals becomes maximum when TX is existing in the vicinity of one of RXs. Figure 5 shows the situation where unwanted signals have the greatest impact on the received signal $B^{(4)}$, which is the signal received by RX4. Since $B^{(2)}$ and $B^{(4)}$ respectively become maximum and minimum in this situation, the negative impact of the unwanted signals on $B^{(4)}$ becomes maximum.

To quantitatively investigate the influence of the unwanted signals on prediction accuracy, we define the prediction error D by

$$D(\delta B) = \left\|\mathbf{P}\left(B^{(1)}, B^{(2)}, B^{(3)}, B^{(4)} + \delta B\right) - \mathbf{P}\left(B^{(1)}, B^{(2)}, B^{(3)}, B^{(4)}\right)\right\|_2, \quad (5)$$

where δB is the received-signal error caused by the unwanted signal contamination.

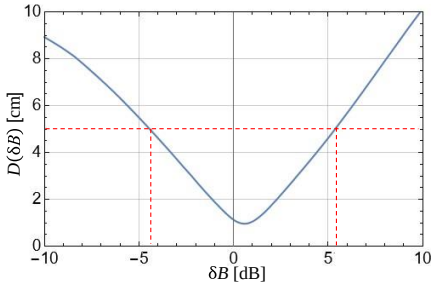

Figure 6. Relationship between the unwanted signal contamination and prediction error.

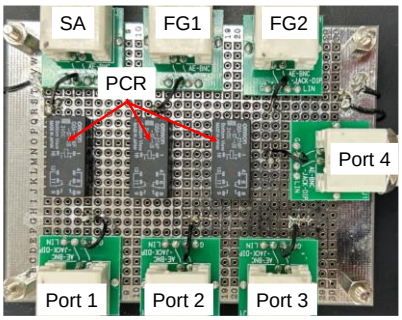

Figure 7. High-isolation relay circuit.

Figure 6 shows $D(\delta B)$ calculated for the situation shown in Figure 5. By considering practical applications, it is desired that the prediction error falls within 5%, which corresponds to $D \leq 5$ cm for our system because the dimension of the target area is 1 m. It is seen from Figure 6 that the received-signals error must satisfy

$$|\delta B| \lesssim 5\ [\text{dB}]. \quad (6)$$

By applying (6) to the situation shown in Figure 5, we obtained the following requirement for a relay circuit.

$$S_{ij} \lesssim -60\ [\text{dB}] \quad (\text{for } i \neq j) \quad (7)$$

4. High-Isolation Relay Circuit

We fabricated a relay circuit that meets the requirement given in (7). A photograph of the relay circuit is shown in Figure 7. A remarkable feature of the newly developed relay circuit is that it is equipped with PCRs. Owing to the PCRs, it becomes possible to greatly improve isolation ratio in comparison with circuits equipped with semiconductor relays (SCRs) in which quite large leakage currents exit.

Figure 8 shows measured *S*-parameters of both the PCR and SCR circuits. The performances of the PCR and SCR circuits are

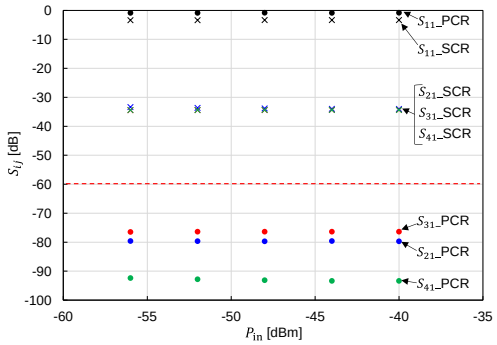

Figure 8. *S*-parameters measured for the PCR and SCR circuits.

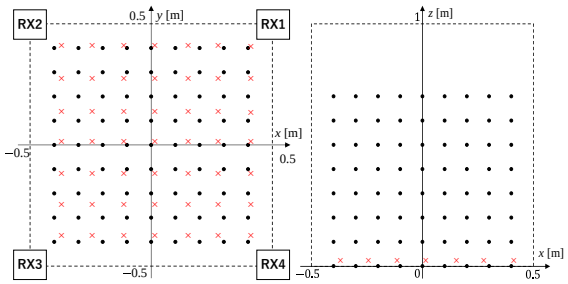

Figure 9. Locations used for training (circle) and validation (cross).

expressed by dots and crosses, respectively. It can be confirmed that the fabricated PCR circuit sufficiently meets the requirement because $S_{ij} \ll -60$ dB for $i \neq j$.

5. Evaluation of Prediction Accuracy of MFP System

We experimentally evaluated the performance of our MFP system with the PCR and SCR circuits. Figure 9 shows TX locations used for training (black dots) and validation (red crosses).

Figures 10(a) and (b) represent prediction errors *d* within *x*-*y* plane ($z = 3$ cm) obtained with our MFP system equipped with the PCR and SCR circuits, respectively. It is confirmed that the prediction accuracy is greatly improved by using the high-isolation relay circuit. Figure 11 shows a histogram of the prediction error *d* obtained with our MFP system equipped with the PCR and SCR circuits. It is seen that the probability of the prediction error *d* being within 5cm, which is the target value of this study, increased from 6.1% to 44.9%. Additionally, the average of *d* was successfully decreased from 24.6 cm to 5.7 cm.

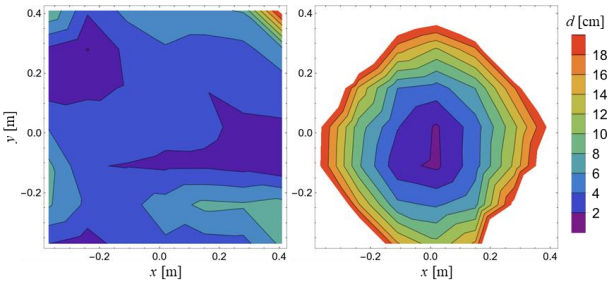

Figure 10. Prediction errors ($z = 3$ cm) obtained with the MFP system equipped with the (a) PCR and (b) SCR circuits.

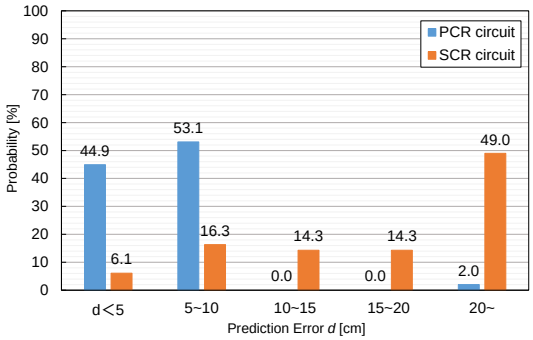

Figure 11. Histogram of prediction errors.

6. Conclusion

We developed a high-isolation relay circuit by using PCRs instead of SCRs. The isolation ratio of the PCR circuit reached 76 dB, which is 42 dB higher than that of the standard SCR circuit. Owing to the high-isolation nature of the PCR circuit, the average prediction error obtained with our MFP system was successfully reduced from 24.6 cm to 5.7 cm.

Acknowledgements

This work was supported in part by JSPS KAKENHI Grant Number 23K03889.

References

[1] A. Nessa *et al.*, IEEE Access **8**, 214945 (2020).

[2] X. Guo *et al.*, IEEE Commun. Surveys Tuts. **22**, 566 (2020).

[3] V. Pasku *et al.*, IEEE Commun. Surveys Tuts. **19**, 2003 (2017).

[4] A. Sheinker *et al.*, IEEE Trans. Instrum. Meas. **68**, 116 (2018).

[5] A. Sasaki and E. Ohta, IEEE Sensors J. **20**, 7292 (2020).

[6] A. Sasaki and K. Fukushima, IEICE Trans. Fundamentals **E105-A**, 994 (2022).

[7] K. Miyaji and A. Sasaki, IEICE Tech. Rep. **PEM2022-14**, 5 (2023). (in Japanese)